Semnan University

Mechanics of Advanced Composite Structures

journal homepage: http://MACS.journals.semnan.ac.ir

Strengthening of Deficient Steel Sections using CFRP Composite under Combined Loading

A.H. Keykha*

Department of Civil Engineering, Islamic Azad University, Zahedan Branch, Zahedan, Iran

KEYWORDS

Deficiencies
SHS steel sections
CFRP strengthening
Numerical methods
Combined loads

ABSTRACT

Recently, strengthening of steel sections using carbon fiber reinforced polymer (CFRP) has come to the attention of many researchers. For various reasons, such structures may be placed under combined loads. The deficiency in steel members may be due to errors caused by construction, fatigue cracking, and other reasons. This study investigated the behavior of deficient square hollow section (SHS) steel members strengthened by CFRP sheets under two types of the combined loads. To study the effect of CFRP strengthening on the structural behavior of the deficient steel members, 17 specimens, 12 of which were strengthened using CFRP sheets, were analyzed. To analyze the steel members, three dimensional (3D) modeling and nonlinear static analysis methods were applied, using ANSYS software. The results showed that CFRP strengthening had an impact on raising the ultimate capacity of deficient steel members and could recover the strength lost due to deficiency, and the impact of CFRP strengthening on rising and recovering the ultimate capacity of the steel members under loading scenario 2 was more than the steel members under scenario 1.

1. Introduction

Nowadays, retrofitting and strengthening of existing steel structures built within the last decades is one of the most important issues considered by structural engineers. Steel structures built in the past often need to be strengthened due to increased life loads, repair due to corrosion, fatigue cracking, and other reasons. In recent years, CFRP composite, as a strengthening material of steel structures, has attracted greater attention. CFRP composite is preferred to strengthen hollow steel sections due to its high tensile strength, high elastic modulus, low weight, and capability to be applied to any shape of structure. Several studies have been carried out to employ CFRP as strengthening material to strengthen steel structures such as flexural strengthening [1-9], pressure strengthening [10-20], tensile strengthening [21], repairing and strengthening of structural members damaged due to fatigue cracking [22-26]. The results of these studies showed that CFRP composites used as a strengthening material improved the performance of the steel structures.

In another study, Abdollahi Chahkand and Zamin Jumaat [27] investigated the structural behavior of CFRP strengthened SHS steel beams in pure torsion. Five SHS steel beams, four of which were strengthened with CFRP sheets in several different strengthening configurations, were tested under torsion. The results of this research showed that, using CFRP composite as a strengthening material improved the plastic and elastic torsional strength of SHS steel beams.

In addition, Zhou *et al*. [28] tested a series of notched steel beams strengthened using a carbon fiber hybrid polymer-matrix composite. The results showed that the load capacity of notched steel beams strengthened with CFRP sheets was increased up to 42.9%. The results also showed that the load capacity of notched steel beams strengthened with Carbon-fiber Hybrid-polymeric Matrix Composite (CHMC) were increased up to 84.9%.

In other research, Keykha [29] investigated the behaviors of deficient steel beams strengthened with CFRP sheets under torsional load. Results showed that the transverse deficiencies had high impact on the torsional capacity of the steel beams. In specimens strengthened using the coverage percentage of CFRP sheet less than 100%, when the number of CFRP layers was more than two, CFRP

*Corresponding author. Tel.: +98-54-33441600; Fax: 98-54-33441099
E-mail address: ah.keykha@iauzah.ac.ir

DOI: 10.22075/MACS.2020.16441.1178
Received 2018-11-08; Received in revised form 2020-01-24; Accepted 2020-03-22

layers were not effective in increasing the torsional capacity of the steel beams. Also, when the coverage percentage of the CFRP sheet was full (100%), the CFRP composite could change the failure modes of the strengthened steel beams.

Moreover, Keykha [30] investigated the behavior of defective curved steel beams strengthened with CFRP composite. The results indicated that the use of CFRP sheets for strengthening defective curved beams could recover the strength lost due to a defect, significantly. The results also indicated that the width of CFRP sheets had an impact on raising the ultimate capacity of defective curved beams.

From past studies, it can be observed that many investigations were conducted on the behavior of the steel members strengthened with CFRP composite, but it seems that there is a lack of understanding about the behavior of deficient hollow steel members under combined loads. Therefore, this study explored the effect of CFRP strengthening on the structural behaviors of deficient hollow steel members under combined loads, using numerical investigations. Loading scenarios applied to the SHS steel members were two types. Loading scenario **1** (Type 1 loading) was the combined compression, torsional and lateral loads, and loading scenario **2** (Type 2 loading) was the combined tensile, torsional and lateral loads. To obtain accurate results, 17 hollow steel members were analyzed (one non-strengthened member without deficiency as a control column, four non-strengthened members with different lengths and orientations of deficiency, and 12 CFRP strengthened members with different lengths and orientations of deficiency. The coverage length and the number of CFRP layers, loading scenarios, lengths, widths and orientations of deficiency were implemented to examine the ultimate capacity of the hollow steel members.

2. Materials properties

In this study, three types of materials were used. Type 1 of the material used was SHS steel. The SHS steel had a dimension of 60 mm × 60 mm. The length and thickness of the used SHS steel were 1600 mm and 3 mm, respectively. Also, the modulus of elasticity, the yield strength, and the ultimate tensile strength of the used SHS steel were 200000 N/mm^2, 240 N/mm^2, and 375 N/mm^2, respectively. These values were extracted from studies conducted by Keykha et al. [18]. Type 2 of the materials used was CFRP sheet. The CFRP sheet used in the present research was SikaWrap-200C. The SikaWrap-200C is a unidirectional carbon fiber. This CFRP had a modulus of elasticity of 230000 N/mm^2 and a tensile strength 3900 N/mm^2. The thickness of this CFRP sheet was 0.111 mm. These values were extracted from studies conducted by Abdollahi Chahkand and Zamin Jumaat [27]. The last material used in this study was adhesive used to paste CFRP sheets to SHS steel. The adhesive used in this study was suggested by the supplier of the CFRP product. The adhesive commonly used for the SikaWrap-200C, was called Sikadur-330. The Sikadur-330 is a two-part adhesive, a hardener and a resin. The Sikadur-330 had a modulus of elasticity about 4500 N/mm^2 and a tensile strength about 30 N/mm^2. These values were retrieved from studies conducted by Keykha et al. [18, 19].

3. Finite element analysis and modeling specimens

3.1. Model description

Nonlinear finite element models were prepared using ANSYS software to investigate the structural behavior of the SHS steel members strengthened with CFRP sheets in length. All models were prepared as steel members of fixed-pinned ends. The dimensions of longitudinal deficiencies were 100 mm × 6 mm × 3 mm or 100 mm × 12 mm × 3 mm (3 mm thickness of the SHS steel). Also, the dimensions of transverse deficiencies were 50 mm × 6 mm × 3 mm or 50 mm × 12 mm × 3 mm. Fig. 1 shows the boundary conditions, types of deficiencies, loading scenarios, and CFRP strengthening scenarios adopted for the study of deficient SHS steel members in this study.

Figure 2, for example, shows a 3D finite element model of the specimen under loading scenario **2** that was strengthened with two CFRP layers and 25% of the CFRP coverage (400 mm CFRP length). Due to the hollow cross-section of the specimens, T-load and P-load (axial loads) were applied as axial compression and tensile stress on cross-section at the pinned end. To apply torsional momentum, four concentrated loads (S-loads) were evenly applied on four sides of the specimens at the pinned end. These loads (S-loads) were applied in order to organize a torsional momentum at the pinned end of the specimens. Also, a concentrated load (Q-load) was applied in mid-span of the SHS steel members (see Fig. 2). All loads gradually increased until the SHS steel members achieved their ultimate capacity.

NOTE: In this research, the percent of CFRP coverage was defined as the ratio of CFRP length to the SHS steel member length multiplied by 100.

3.2. Finite element analysis

To simulate the SHS steel members, the full three-dimensional modeling and nonlinear static analysis methods were applied. The SHS steel member, CFRP sheet, and adhesive were simulated using the 3D solid triangle elements (ten-nodes 187). Nonlinear static analysis was carried out to achieve the characteristics of failures in the steel members.

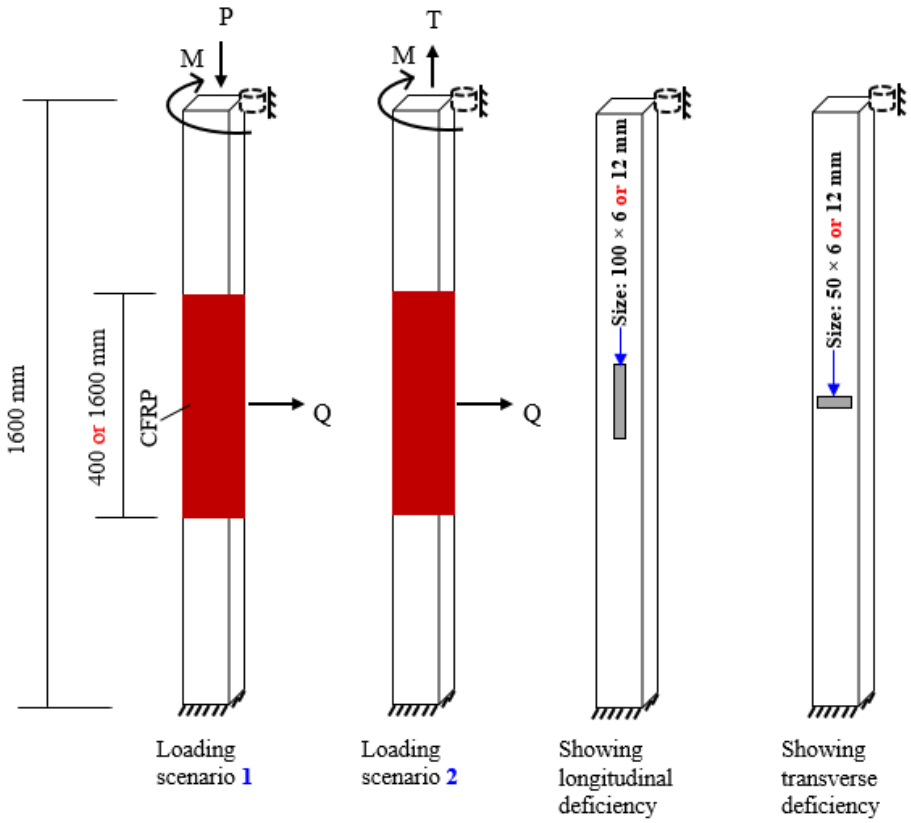

Fig. 1. Details of the strengthened specimens and deficiencies (not to scale).

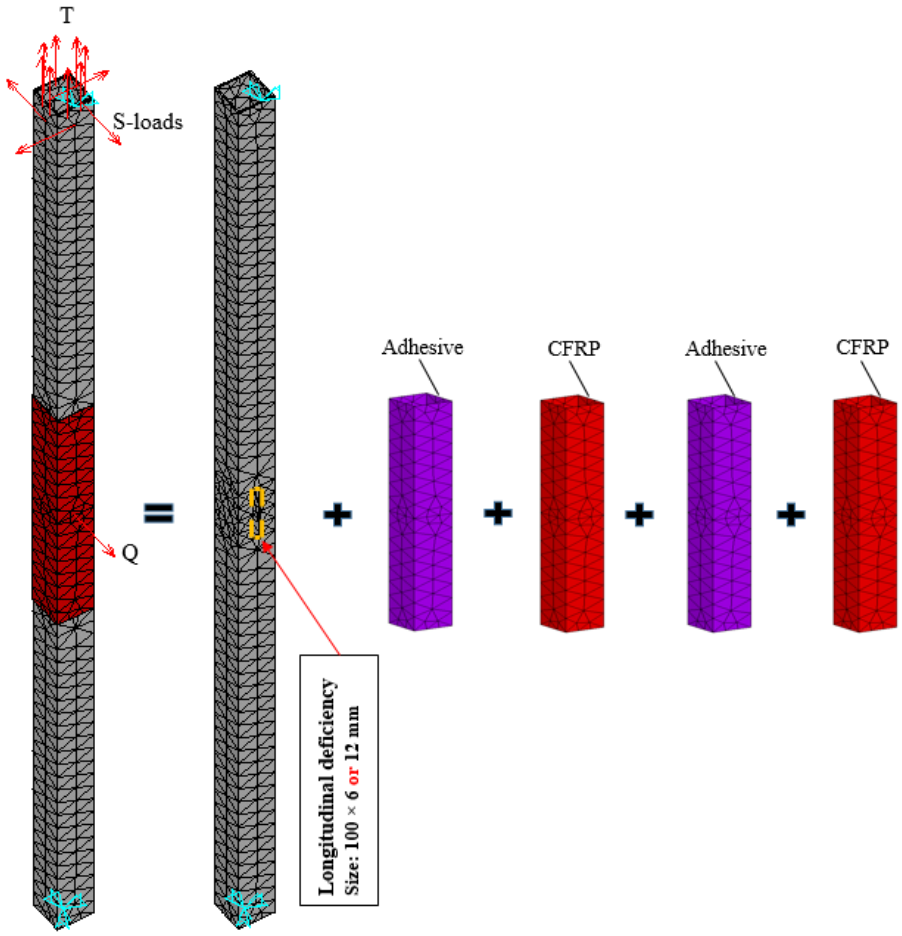

Fig. 2. FE-modeling details of a strengthened specimen having a longitudinal deficiency.

In this case, the load was incrementally applied until the plastic strain in an element reached its ultimate limit. Subsequently, linear and nonlinear properties of materials were defined. The CFRP sheet material properties were defined as linear and orthotropic because CFRP materials had linear properties which were unidirectional. Also, the adhesive was defined as linear because the adhesive used had linear properties [31]. In addition, the SHS steel members were defined as the materials having nonlinear properties. For meshing, map meshing was used. Therefore, the solid element of 187 with mesh size of 25 was used for analysis of the specimens. In previous research, this element and meshing were used by Keykha [31], showing a good accuracy between the numerical and experimental results.

3.3. Validity of software results

It was necessary to validate the software calculations. In this study, the software results were validated and calibrated by the experimental results of Abdollahi Chahkand and Zamin Jumaat [27] and Keykha *et al*. [18, 19]. For the analysis of the specimens, as mentioned in the previous section, the solid element of 187 with the mesh size of 25 was used. From the studies conducted by Abdollahi Chahkand and Zamin Jumaat [27] and Keykha *et al*. [18, 19], the ultimate capacity of the Type 1 and C0 specimens, were obtained from experimental, theoretical, and numerical analysis (see Table 1). As mentioned in the Introduction section, Abdollahi Chahkand and Zamin Jumaat [27] carried out an experimental and a theoretical study on the behavior of CFRP strengthened SHS steel beams in pure torsion. As shown in Table 1, good accuracy is seen between the experimental and numerical results. Fig. 3 shows experimental model and finite element model of specimen Type 1.

3.4. Labeling specimens

The steel members included one control specimen, four non-strengthened specimens with different lengths, widths, and orientations of deficiency, and 12 specimens with different lengths and orientations of deficiency strengthened with two and four CFRP layers applied on all four sides of the steel members. The control specimen was analyzed without strengthening to determine the rate of the ultimate capacity increase in the strengthened steel members. To easily identify each specimen, steel members were designated PTMQ0, PTMQ0-T6, PTMQ0-T12, PTMQ0-L6, PTMQ0-L12, PTMQ2-25-T6, PTMQ4-25-T6, PTMQ2-100-T6, PTMQ2-25-T12, PTMQ4-25-T12, PTMQ2-100-T12, PTMQ2-25-L6, PTMQ4-25-L6, PTMQ2-100-L6, PTMQ2-25-L12, PTMQ4-25-L12, and PTMQ2-100-L12, respectively.

For example, the designation of PTMQ2-100-T12 indicates that it is the steel member with a transverse deficiency that is strengthened by two CFRP layers fully wrapped around it. In this specimen, the transverse deficiency width was 12 mm. The designation of PTMQ2-100-L6 indicates that it is the steel member with a longitudinal deficiency that is strengthened by two CFRP layers fully wrapped around it. In this specimen, the longitudinal deficiency width is 6 mm. The designation of PTMQ4-25-L6 indicates that it is a steel member strengthened by four layers and 25% of the CFRP coverage wrapped around it with a longitudinal deficiency, its longitudinal deficiency width is 6 mm. The designation of PTMQ0-T6 specifies that it is a steel member non-strengthened with a transverse deficiency, its transverse deficiency width is 6 mm. Similarly, the specimen PTMQ0-L12 specifies that it is a steel member non-strengthened with a longitudinal deficiency that the longitudinal deficiency width is 12 mm. The control steel member was designated as PTMQ0.

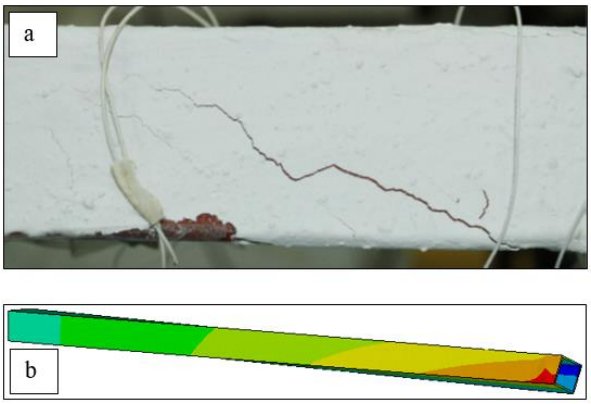

Fig. 3. Specimen Type 1: (a) experimental model [27], (a) finite element model.

Table 1. Comparison of the ultimate capacity of specimens in laboratory, theoretical, and numerical analysis.

Specimen label	Experimental capacity	Theoretical capacity	Numerical capacity	Error (%)
Type 1	2.782 (kN.m)	2.720 (kN.m)	2.784 (kN.m)	0.07
C0	31.80 (kN)	32.86 (kN)	32.060 (kN)	0.82

4. Results and discussion

4.1. The results of the ultimate capacity of the specimens under loading scenario 1

Various structures may be placed under combined loads in their lifetime. The deficiency in steel members may be created due to errors caused by construction, fatigue cracking, and other reasons. According to the author's information, there is no independent article that has investigated the behaviors of the CFRP strengthened deficient SHS steel members under combined loads. Therefore, this research investigated the CFRP strengthened steel members under combined loads.

Table 2 shows the results of numerical analysis of the specimens without CFRP strengthening or with two or four CFRP layers. These specimens were analyzed under loading scenario 1. The coverage length of Type 1 CFRP strengthening was 1600 mm (100% of the length of steel members) and another Type was 400 mm (25% of the length of steel members). The center position of CFRP sheet was in the center of the steel member. In Table 2, the ultimate capacity and the recovery percentage in the ultimate capacity of specimens are shown. To calculate the ultimate capacity and increase percentage or decrease in the ultimate capacity of specimens, the ultimate capacity of all specimens was compared with the ultimate capacity of the reference specimen (PTMQ0), while for a calculated recovery percentage in the ultimate capacity of specimens, the ultimate capacity of the strengthened specimens was compared with the ultimate capacity of the deficient specimen in its category.

For example, the recovery percentage in the ultimate capacity of the specimen PTMQ2-25-T6 was compared with the specimen PTMQ0-T6. As shown in Table 2, in this specimen (PTMQ2-25-T6), the recovery percentage in the ultimate compression capacity ($\mathbf{P_U}$), the ultimate lateral load capacity ($\mathbf{Q_U}$), and the ultimate torsional capacity ($\mathbf{M_T}$) was 16.26%, 16.24%, and 16.32%, respectively. Also, the increase percentage in the ultimate capacity of the specimen PTMQ2-100-L12 was compared with the specimen PTMQ0. In this specimen (PTMQ2-100-L12), the increase percentage in the ultimate compression capacity, the ultimate lateral load capacity, and the ultimate torsional capacity was 15.01%, 100.69%, and 55.59%, respectively. The results showed, when the deficiency was located in the direction of the length (the longitudinal deficiency) and the width (the transverse deficiency) of the steel member, the deficiency had an impact on the decrease in the ultimate capacity of the steel members. In the specimens having deficiency, as shown in Table 2, CFRP had considerable impact on the ultimate capacity of these specimens. The results also showed, when the deficiency was located in the direction of the width of the steel member, the deficiency had high impact on the decrease in the ultimate capacity of the steel members. Therefore, in the steel member with a transverse deficiency, CFRP had a considerable impact on the increase in the ultimate capacity of the specimen.

Table 2. Analysis results of the specimens.

Designation of specimen	No. of CFRP layers	CFRP coverage (%)	P_U: Compression capacity (kN)	Q_U: Lateral capacity (kN)	M_T: Torsional capacity (kN.m)	% of recovery in compression capacity	% of recovery in lateral capacity	% of recovery in torsional capacity
PTMQ0	0	0	68.205	7.977	0.957	NA	NA	NA
PTMQ0-T6	0	0	65.062	7.610	0.913	NA	NA	NA
PTMQ0-T12	0	0	59.187	7.297	0.876	NA	NA	NA
PTMQ0-L6	0	0	67.237	7.864	0.943	NA	NA	NA
PTMQ0-L12	0	0	65.117	7.412	0.933	NA	NA	NA
PTMQ2-25-T6	2	25	75.644	8.847	1.062	16.26	16.24	16.32
PTMQ4-25-T6	4	25	75.845	9.069	1.088	16.57	19.17	19.17
PTMQ2-100-T6	2	100	77.005	15.674	1.458	18.36	105.97	59.69
PTMQ2-25-T12	2	25	75.582	8.840	1.061	27.70	21.15	21.12
PTMQ4-25-T12	4	25	75.768	8.979	1.077	28.01	23.05	22.95
PTMQ2-100-T12	2	100	76.414	14.003	1.288	29.11	91.90	47.03
PTMQ2-25-L6	2	25	75.924	8.880	1.066	12.92	12.92	13.04
PTMQ4-25-L6	4	25	76.687	8.969	1.076	14.05	13.94	14.10
PTMQ2-100-L6	2	100	78.667	16.062	1.494	17.00	104.25	58.43
PTMQ2-25-L12	2	25	75.920	8.878	1.064	16.59	19.78	14.04
PTMQ4-25-L12	4	25	76.640	8.945	1.071	17.70	20.68	14.79
PTMQ2-100-L12	2	100	78.441	16.009	1.489	20.46	115.99	59.59

In strengthened specimens, when the composite coverage percentage was less than 100% and the number of CFRP layers was 4, CFRP was not effective in the ultimate capacity of the strengthened specimens. The Lack of increase in the ultimate capacity was due to the fact that these specimens had recovered with two CFRP layers. For the strengthened specimens, when the CFRP coverage was full, CFRP was more effective in the ultimate capacity of these specimens. In this study, the maximum recovery percentage in the ultimate compression capacity happened for the specimen PTMQ2-100-T12 which was 29.11%. Moreover, the maximum recovery percentage in the ultimate lateral load capacity happened for the specimen PTMQ2-100-L12 which was 115.99%. Also, the maximum recovery percentage in the ultimate torsional capacity happened for the specimen PTMQ2-100-T6 and that was 59.69% (see Table 2). The maximum increase percentage in the ultimate compression capacity, the ultimate lateral load capacity, and the ultimate torsional capacity happened for the specimen PTMQ2-100-L6 and they were 15.34%, 101.35%, and 56.11%, respectively.

4.2. Comparison of Von Mises stress in the specimens under loading scenario 1

All specimens were subjected to combined axial compression, lateral and torsional load until failure occurred. In non-strengthened specimens and all specimens strengthened using two full layers of CFRP sheets, the maximum Von Mises stress was observed near the pinned end of these specimens (as shown in Figs. 4a and b).

In the rest of the specimens (all specimens strengthened with the coverage percentage of CFRP composite less than 100%) the position of maximum Von Mises stress was observed in the deficiency location (as shown in Figs. 4c and d).

4.3. The results of the ultimate capacity of the specimens under loading scenario 2

Table 3 shows the results of numerical analysis of the specimens under loading scenario **2** that were without CFRP strengthening or were strengthened with two or four CFRP layers. Definitions of the coverage length, CFRP position, the increase percentage or decrease in the ultimate capacity, and the recovery percentage in the ultimate capacity of the specimens were the same as those defined in section 4.1. Therefore, the recovery percentage in the ultimate capacity of the specimen PTMQ2-25-T6 was compared with the specimen PTMQ0-T6. As shown in Table 3, in this specimen (PTMQ2-25-T6), the recovery percentage in the ultimate tensile capacity ($\mathbf{T_U}$), the ultimate torsional capacity ($\mathbf{M_T}$), and the ultimate lateral load capacity ($\mathbf{Q_U}$) were 50.99%, 60.64%, and 61.77%, respectively. Also, for example, the increase percentage in the ultimate capacity of the specimen PTMQ2-100-L12 was compared with the specimen PTMQ0.

Table 3. Analysis results of the specimens under loading scenario 2.

Designation of specimen	No. of CFRP layers	CFRP coverage (%)	T_U: Tensile capacity (kN)	M_T: Torsional capacity (kN.m)	Q_U: Lateral capacity (kN)	% of recovery in tensile capacity	% of recovery in torsional capacity	% of recovery in lateral capacity
PTMQ0	0	0	90.134	2.704	22.533	NA	NA	NA
PTMQ0-T6	0	0	55.677	1.570	12.989	NA	NA	NA
PTMQ0-T12	0	0	51.918	1.558	12.900	NA	NA	NA
PTMQ0-L6	0	0	77.711	2.322	19.953	NA	NA	NA
PTMQ0-L12	0	0	77.463	2.233	19.441	NA	NA	NA
PTMQ2-25-T6	2	25	84.050	2.522	21.012	50.99	60.64	61.77
PTMQ4-25-T6	4	25	84.653	2.680	21.663	52.04	70.70	66.78
PTMQ2-100-T6	2	100	185.719	5.757	61.906	233.57	266.69	376.60
PTMQ2-25-T12	2	25	82.096	2.400	20.750	58.13	54.04	60.85
PTMQ4-25-T12	4	25	82.910	2.499	20.778	59.69	60.40	61.15
PTMQ2-100-T12	2	100	173.275	3.967	42.655	233.75	154.62	230.66
PTMQ2-25-L6	2	25	88.626	2.909	21.906	14.05	25.28	9.79
PTMQ4-25-L6	4	25	88.851	2.925	22.213	14.34	25.97	11.33
PTMQ2-100-L6	2	100	204.896	6.352	68.299	163.66	173.56	242.30
PTMQ2-25-L12	2	25	86.926	2.618	21.482	12.22	17.24	10.50
PTMQ4-25-L12	4	25	87.899	2.817	21.875	13.47	26.15	12.52
PTMQ2-100-L12	2	100	199.945	6.198	66.648	158.12	177.56	242.82

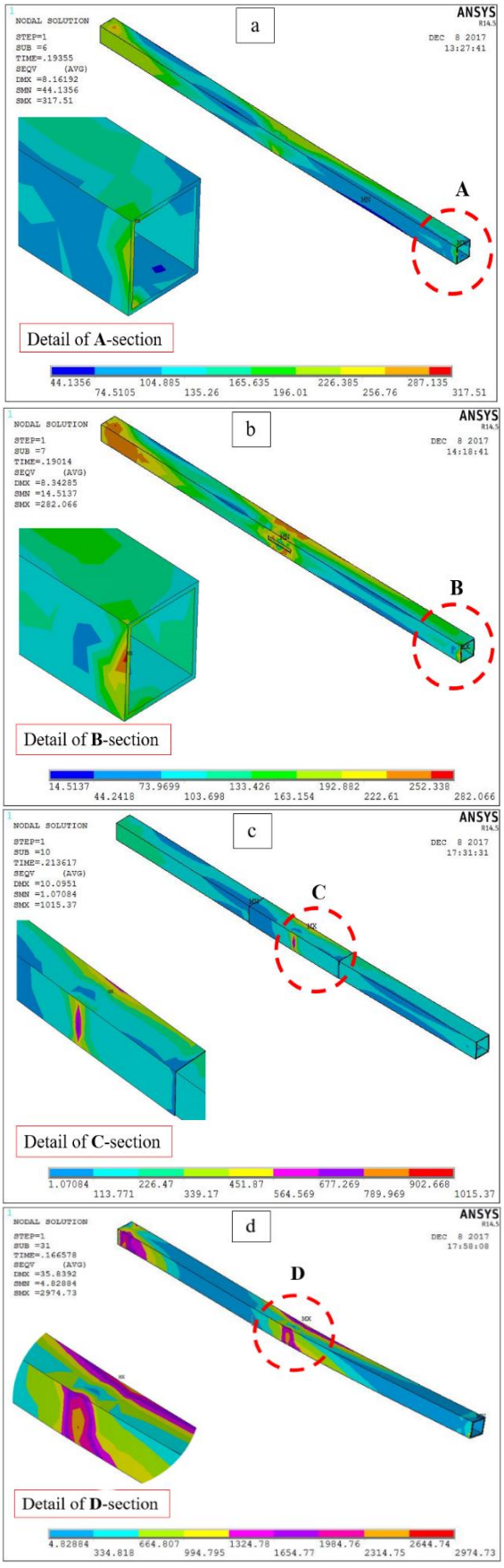

Fig. 4. Comparison of the Von Mises stress in the specimens under loading scenario **1**: (a) specimen PTMQ0, (b) specimen PTMQ0-L12, (c) specimen PTMQ2-25-T6, (d) specimen PTMQ2-100-T12.

In this specimen (PTMQ2-100-L12), the increase percentage in the ultimate tensile capacity, the ultimate torsional capacity, and the ultimate lateral load capacity were 121.83%, 129.22%, and 195.78%, respectively. The results showed, when the deficiency was located in the direction of the length (the longitudinal deficiency) and the width (the transverse deficiency) of the steel member, the deficiency had an impact on the decrease in the ultimate capacity of the steel members. In these specimens, as shown in Table 3, CFRP had considerable impact on the ultimate capacity. The results also showed that, when the deficiency was located in the direction of the width of steel member, the deficiency had a high impact on the decrease in the ultimate capacity of the steel members. Therefore, in the steel member with a transverse deficiency, CFRP had a considerable impact on the increase of the ultimate capacity of the specimen.

Similar to the loading scenario 1, in the loading scenario 2, when the composite coverage percentage in the strengthened specimen was less than 100% and the number of CFRP layers was 4, CFRP was not effective in the ultimate capacity of the strengthened specimens. The Lack of the increase in the ultimate capacity was due to the fact that these specimens had recovered with two CFRP layers. For the strengthened specimens, when the CFRP coverage was full (100%), CFRP was more effective in the ultimate capacity of these specimens. In this study, the maximum recovery percentage in the ultimate tensile capacity happened for the specimen PTMQ2-100-T12 and was 233.75%. The maximum recovery percentage in the ultimate torsional capacity and the ultimate lateral load capacity happened for the specimen PTMQ2-100-T6 and were 266.69% and 376.60%, respectively (see Table 3). The maximum increase percentage in the ultimate tensile capacity, the ultimate torsional capacity, and the ultimate lateral load capacity happened for the specimen PTMQ2-100-L6 and were 127.32%, 134.91%, and 203.11%, respectively.

The reason for this result is because the CFRP materials have high tensile strengths, and the loading scenario 2 included the tensile load, so CFRP sheets are more effective in the loading scenario 2 than the loading scenario 1.

4.4. Comparison of Von Mises stress in the specimens under loading scenario 2

In this loading scenario (loading scenario 2), all specimens were subjected to combined tensile, lateral and torsional load until failure happened. In the control steel member (the specimen PTMQ0), the maximum Von Mises stress was observed near the pinned end this specimen (see Fig. 5a). In the rest of the specimens, the non-strengthened specimen and all specimens strengthened using

CFRP sheets, the position of maximum Von Mises stress was observed in the deficiency location (as shown in Figs. 5b- d).

Comparison of Tables 2 and 3 shows that, the CFRP sheets in loading scenario 2 are more effective in increasing and recovering the ultimate capacity of the steel members than loading scenario 1.

5. Conclusions

In this study, 17 specimens were analyzed (one non-strengthened specimen without deficiency as a control column, four non-strengthened specimens with different lengths, widths, and orientations of deficiencies, and 12 specimens with different lengths and orientations of deficiencies that were strengthened with CFRP layer). The CFRP sheets with two types of length (400 mm and 1600 mm) and number of CFRP layers (two and four layers) were wrapped around the SHS steel members having initial longitudinal or transverse deficiencies. Based on results obtained, the ultimate capacity, the increase percentage in the ultimate capacity, the recovery percentage in the ultimate capacity, and the comparison of the Von Mises stress in the SHS steel members (with an initial deficiency or without deficiency) were discussed, and the following conclusions were drawn:

- The initial deficiencies in the non-strengthened SHS steel members decreased the ultimate carrying capacity of these steel members. When the deficiency was located in the direction of the width of the steel member (the transverse deficiency), the deficiency had a high impact on the decrease in the ultimate capacity of the steel members. In loading scenario 1, the maximum decrease percentage in the ultimate compression capacity, the ultimate lateral load capacity, and the ultimate torsional capacity happened for the specimen PTMQ0-T12 and were 13.22%, 8.52%, and 8.46%, respectively. Also, in loading scenario 2, the maximum decrease percentage in the ultimate tensile capacity, the ultimate torsional capacity, and the ultimate lateral load capacity happened for the specimen PTMQ0-T12 and were 42.40%, 42.38%, and 42.75%, respectively.
- The width of deficiency in the SHS steel members with the transverse deficiency was more effective in the decrease of the ultimate capacity of the steel members than in the SHS steel members with the longitudinal deficiency.
- In the strengthened SHS steel members having initial deficiencies, CFRP had a considerable impact on the increase of the ultimate capacity of these specimens.

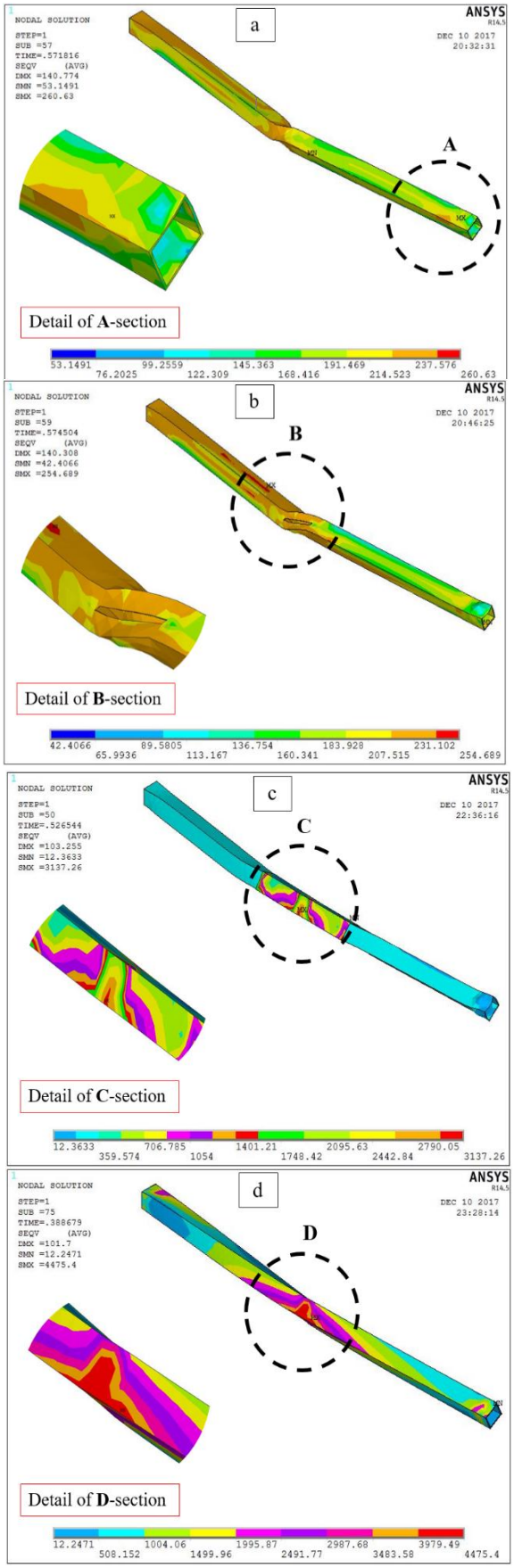

Fig. 5. Comparison of the Von Mises stress in the specimens under loading scenario **2**: (a) specimen PTMQ0, (b) specimen PTMQ0-L6, (c) specimen PTMQ2-25-T12, (d) specimen PTMQ2-100-T12

- In specimens strengthened using CFRP sheets, when the deficiency was located in the direction of the width of the steel member, the CFRP sheets were more effective in the increasing and recovering of the ultimate capacity of the steel members than in the case when the deficiency was located in the direction of the length of the steel member.
- When the coverage percentage of the CFRP composite was less than 100%, the number of CFRP layers exceeding four was not effective in the ultimate capacity of the steel members. The Lack of the increase in the ultimate capacity was due to the fact that the specimens strengthened with the coverage percentage of the CFRP composite less than 100% had recovered with two CFRP layers.
- In loading scenario 1, the maximum recovery percentage in the ultimate compression capacity happened for the specimen PTMQ2-100-T12 which was 29.11%. The maximum recovery percentage in the ultimate lateral load capacity happened for the specimen PTMQ2-100-L12 and was 115.99%. Also, the maximum recovery percentage in the ultimate torsional capacity happened for the specimen PTMQ2-100-T6 and was 59.69%. The maximum increase percentage in the ultimate compression capacity, the ultimate lateral load capacity, and the ultimate torsional capacity happened for the specimen PTMQ2-100-L6 and were 15.34%, 101.35%, and 56.11%, respectively.
- In loading scenario 2, the maximum recovery percentage in the ultimate tensile capacity happened for the specimen PTMQ2-100-T12 and was 233.75%. In addition, the maximum recovery percentage in the ultimate torsional capacity and the ultimate lateral load capacity happened for the specimen PTMQ2-100-T6 and were 266.69% and 376.60%, respectively. Also, the maximum increase percentage in the ultimate tensile capacity, the ultimate torsional capacity, and the ultimate lateral load capacity happened for the specimen PTMQ2-100-L6 and were 127.32%, 134.91%, and 203.11%, respectively.
- In loading scenario 1, in non-strengthened specimens and all specimens strengthened using two full layers of CFRP sheets, the maximum Von Mises stress was observed near the pinned end these specimens. In all specimens strengthened with the coverage percentage of CFRP composite less than 100%, the position of maximum Von Mises stress was observed in the deficiency location. In loading scenario 2, in the control specimen, the maximum Von Mises stress was observed near the pinned end this specimen. In the rest of the specimens, the non-strengthened specimen and all specimens strengthened using CFRP sheets, the position of maximum Von Mises stress was observed in the deficiency location.
- Generally, the results obtained for the specimens under loading scenarios 1 and 2 showed that, the CFRP sheets in loading scenario 2 were more effective in increasing and recovering the ultimate capacity of the steel members than loading scenario 1. The reason for this result was because the CFRP materials had high tensile strengths, and on the other hand, due to the fact that loading scenario 2 included the tensile load as well, therefore CFRP sheets were more effective in the loading scenario 2 than the loading scenario 1.

References

[1] Sundarraja MC, Prabhu GG. Flexural behavior of CFST members strengthened using CFRP composites. Steel and Composite Structures 2013; 15(6): 623-643.
[2] Idris Y, Ozbakkaloglu T. Flexural behavior of FRP-HSC-steel composite beams. Thin-Walled Structures 2014; 80: 207-216.
[3] Teng JG, Fernando D, Yu T. Finite element modelling of debonding failures in steel beams flexurally strengthened with CFRP laminates. Engineering Structures 2015; 86: 213-224.
[4] Al Zand AW, Badaruzzaman WHW, Mutalib AA, Qahtan AH. Finite element analysis of square CFST beam strengthened by CFRP composite material. Thin-Walled Structures 2015; 96: 348-358.
[5] Kabir MH, Fawzia S, Chan THT, Gamage JCPH, Bai JB. Experimental and numerical investigation of the behavior of CFRP strengthened CHS beams subjected to bending. Engineering Structures 2016; 113: 160-173.
[6] Elchalakani M. Plastic collapse analysis of CFRP strengthened and rehabilitated degraded steel welded RHS beams subjected to combined bending and bearing. Thin-Walled Structures 2014; 82: 278-295.
[7] Andre A, Haghani R, Biel A. Application of fracture mechanics to predict the failure load of adhesive joints used to bond CFRP laminates to steel members. Construction and Building Materials 2012; 27(1): 331-340.
[8] Keykha A H. Numerical investigation on the behavior of SHS steel frames strengthened using CFRP. Steel and Composite Structures 2017; 24 (5): 561-568.
[9] Keykha AH. Numerical investigation of continuous hollow steel beam strengthened using CFRP. Structural Engineering and Mechanics 2018; 66 (4): 439-444.
[10] Ozbakkaloglu T, Xie T. Behavior of steel fiber-reinforced high-strength concrete-filled FRP tube columns under axial compression. Engineering Structures 2015; 90: 158-171.

[11] Devi U, Amanat KM. Non-linear finite element investigation on the behavior of CFRP strengthened steel square HSS columns under compression. International Journal of Steel Structures 2015; 15(3): 671-680.
[12] Kumar AP, Senthil R. Axial Behavior of CFRP-Strengthened Circular Steel Hollow Sections. Arabian Journal for Science and Engineering 2016; 41(10): 3841-3850.
[13] Kalavagunta S, Naganathan S, Mustapha KNB. Axially loaded steel columns strengthened with CFRP. Jordan Journal of Civil Engineering 2014; 8(1): 58-69.
[14] Alam MI, Fawzia S. Numerical studies on CFRP strengthened steel columns under transverse impact. Composite Structures 2015; 120: 428-441.
[15] Fanggi BAL, Ozbakkaloglu T. Square FRP–HSC–steel composite columns: Behavior under axial compression. Engineering Structures 2015; 92: 156-171.
[16] Park JW, Yeom HJ, Yoo JH. Axial loading tests and FEM analysis of slender square hollow section (SHS) stub columns strengthened with carbon fiber reinforced polymers. International Journal of Steel Structures 2013; 13(4): 731-743.
[17] Ritchie A, MacDougall C, Fam A. Enhancing buckling capacity of slender s-section steel columns around strong axis using bonded carbon fiber plates. Journal of Reinforced Plastics and Composites 2015; 34(10): 771–781.
[18] Keykha AH, Nekooei M, Rahgozar R. Experimental and theoretical analysis of hollow steel columns strengthening by CFRP. Civil Engineering Dimension 2015; 17(2): 101-107.
[19] Keykha AH, Nekooei M, Rahgozar R. Analysis and strengthening of SHS steel columns using CFRP composite materials. Composites: Mechanics, Computations, Applications. An International Journal 2016; 7(4): 275–290.
[20] Keykha AH. Numerical investigation of SHS steel beam-columns strengthened using CFRP composite. Steel and Composite Structures 2017; 25 (5): 593-601.
[21] Al-Zubaidy H, Al-Mahaidi R, Zhao XL. Finite element modelling of CFRP/steel double strap joints subjected to dynamic tensile loadings. Composite Structures 2013; 99: 48-61
[22] Colombi P, Fava G, Sonzogni L. Fatigue Behavior of Cracked Steel Beams Reinforced by Using CFRP Materials. Procedia Engineering 2014; 74: 388-391.
[23] Ahn JH, Kainuma S, Yasuo F, Takehiro I. Repair method and residual bearing strength evaluation of a locally corroded plate girder at support. Engineering Failure Analysis 2013; 33: 398-418.
[24] Ghafoori E, Motavalli M, Botsis J, Herwig A, Galli M. Fatigue strengthening of damaged metallic beams using prestressed unbonded and bonded CFRP plates. International Journal of Fatigue 2012; 44: 303-315.
[25] Jiao H, Mashiri F, Zhao XL. A comparative study on fatigue behavior of steel beams retrofitted with welding, pultruded CFRP plates and wet layup CFRP sheets. Thin-Walled Structures 2012; 59: 144-152.
[26] Kim YJ, Harries KA. Fatigue behavior of damaged steel beams repaired with CFRP strips. Engineering Structures 2011; 33(5):1491-1502.
[27] Abdollahi chakand N, Zamin Jumaat M. Experimental and theoretical investigation on torsional behavior CFRP strengthened square hollow steel section. Thin-Walled Structures 2013; 68: 135-140.
[28] Zhou H, Attard TL, Wang Y, Wang JA, Ren F. Rehabilitation of notch damaged steel beams using a carbon fiber reinforced hybrid polymeric-matrix composite. Composite Structures 2013; 106: 690-702.
[29] Keykha AH. 3D finite element analysis of deficient hollow steel beams strengthened using CFRP composite under torsional load. Composites: Mechanics, Computations, Applications. An International Journal 2017; 8 (4): 1-11.
[30] Keykha AH. Behavior of defective curved steel beams strengthened by a CFRP composite. Mechanics of Composite Materials 2019; 55(4): 525-534.
[31] Keykha AH. CFRP strengthening of steel columns subjected to eccentric compression loading. Steel and Composite Structures 2017; 23 (1): 87-94.